ORGANIC CHEMISTRY FRONTIERS

RESEARCH ARTICLE

View Article Online
View Journal | View Issue

Published on 17 March 2025. Downloaded by FUZHOU UNIVERSITY LIBRARY on 10/20/2025 8:49:18 AM.

Check for updates

Cite this: *Org. Chem. Front.*, 2025, **12**, 3409

Dibenzo-12-crown-4 group as a pore-forming enhancer for anion transport†

Jisen Fan, Yingxue Xu, Jie Shen, Wenju Chang* and Huaqiang Zeng *

Received 4th January 2025,
Accepted 14th March 2025

DOI: 10.1039/d5qo00025d

rsc.li/frontiers-organic

Dysregulation of anion transport is implicated in a range of diseases, including congenital myotonia, cystic fibrosis, and hereditary renal lithiasis. While natural anion channels exhibit highly complex and intricate structures, the development of structurally simpler artificial channels holds promise for advancing the understanding of anion transport mechanisms and offering novel therapeutic approaches. Among emerging strategies, the use of side chain–side chain interactions to construct artificial anion channels has shown significant potential, particularly through the application of flexible hydrocarbon side chains to facilitate pore formation. Building on this concept, we introduce a novel scaffold—the dibenzo-12-crown-4 group—which unexpectedly acts as a pore-forming enhancer, rather than a cation transporter. By strengthening side chain–side chain interactions, this group promotes the formation of sizable pores within lipid bilayers, selectively and efficiently transporting anions, rather than cations. Notably, channel **A10** exhibits a remarkable high Cl^-/K^+ selectivity ratio of 17 while showcasing a distinct hierarchy in anion conductivity: $ClO_4^- > I^- > NO_3^- > Br^- > Cl^-$.

Introduction

Chloride ions, being the most abundant anions in the human body, play crucial roles in various physiological processes.[1–3] Chloride ion channels are widely distributed across different cellular membranes, including those of lysosomes, mitochondria, and the endoplasmic reticulum.[4–6] Dysfunction in these chloride ion channels can lead to numerous diseases, such as congenital myotonia, recessive generalized myotonia, cystic fibrosis, and hereditary renal lithiasis.[7–9] Due to the complex structure of natural chloride ion channels, it is imperative to develop structurally simpler artificial chloride ion channels. This will not only facilitate the study of anion transport mechanisms but also provide potential therapeutic approaches for diseases caused by chloride ion channel dysfunction.[10–17]

Forming pores in lipid bilayers has emerged as a promising strategy for constructing artificial ion channels.[17–26] Biomimetic chemists have developed many innovative approaches to pore formation, each leveraging unique molecular interactions and conformations. These strategies include Wolynes' helical stacking driven by solvophobic interactions,[18] β-barrel pores composed of rigid-rod molecules by Matile,[23,27,28] tail-to-tail assembly of two cholic-containing molecules and steroid-modified biscarbamate by Kobuke,[29,30] barrel stave configurations formed by two dendrimers involving vertical steroids by Regen,[31] face-to-face stacking of aromatic oligoamide macrocycles by Gong,[24,32,33] and a folded multiblock amphiphilic oligomer consisting of alternating hydrophilic and hydrophobic units by Kinbara.[20–22] Other notable approaches include the benzohydrazide-based core by Talukdar,[17] cholesterol-stabilized toroidal nanopores by Zeng[25] and adaptive cholesterol-containing nanopores driven by concentration by Ren.[34] The rosette-conformation derived from dendritic folate by Matile,[35] a glycol-based core by Talukdar,[36] G-quartets by Dash and Davis,[26,37,38] and fused G-C bases by Wanunu[39] are also effective in creating pores in lipid bilayers. Additionally, H-bond-rigidified helical foldamers, constructed from pyridine, pyridone, and their derivatives by Zeng,[40–46] quinoline by Liu,[47] and pyridine-urea oligomers by Wu,[48] are capable of forming pores that selectively transport protons, alkali metal ions, anions and water. Lastly, pore formation through repulsive-induced aromatic foldamers composed of oxadiazole and pyridine or its derivatives by Dong and Liu offers efficient and selective ion transport.[49–52]

In addition to these inspiring approaches to pore construction, an emerging strategy focuses on leveraging flexible hydrocarbon side chain–side chain interactions to create pores for anion transport across membranes.[53–59] Expanding on this strategy, we demonstrate here that a rigid dibenzo-12-crown-4 group does not function as a cation-binding and -transporting unit. Instead, it unexpectedly serves as a pore-forming enhancer, reinforcing side chain–side chain interactions to create membrane-active pores for anion transport.

College of Chemistry, Fuzhou University, Fuzhou, Fujian 350108, China.
E-mail: wenjuchang@fzu.edu.cn, hqzeng@fzu.edu.cn

† Electronic supplementary information (ESI) available. See DOI: https://doi.org/10.1039/d5qo00025d

Published on 17 March 2025. Downloaded by FUZHOU UNIVERSITY LIBRARY on 10/20/2025 8:49:18 AM.

Results and discussion

Recently, we demonstrated that monopeptides appended with three distinct types of side chains can self-assemble into one-dimensionally aligned, doubly H-bonded stacks. These stacks undergo a secondary self-assembly process driven by side chain–side chain interactions, resulting in the formation of innovative oil-gelling scaffolds (Fig. 1a).[60–63] By incorporating ion-binding units into this monopeptide scaffold (*e.g.*, **6V10** and **5F8**, Fig. 1b), the resulting one-dimensional ensembles span the hydrophobic region of the membrane, forming transmembrane pathways that facilitate the transport of ions or even amino acids.[64–69]

^{1}H NMR dilution studies from 80 mM to 1 mM reveal changes in the chemical shift of two amide protons involved in forming intermolecular H-bonds ranging from 0.30 to 0.50 ppm for both **A10** and **B10** (Fig. S1†). These concentration-dependent changes indicate that **A10** and **B10** can self-assemble through H-bonds in non-polar solvents. Additionally, SEM results confirm that **A10** and **B10** are capable of forming organogels in non-polar solutions (Fig. S2†).

As illustrated in Fig. 1c, we hypothesized that molecules **A*n*–C*n*** (n = 6, 8, 10, 12), featuring a Li^+-binding 12-crown-4 unit, might be capable of transporting Li^+ ions across the membrane after assembling into one-dimensional H-bonded stacks.

The ion-transport activity of **A*n*–C*n*** was evaluated using a pH-sensitive HPTS assay. In this assay, pH-sensitive HPTS dye (100 μM) and NaCl (100 mM) at pH 7 were encapsulated inside large unilamellar vesicles (LUVs), which were then diluted into a 100 mM KCl buffer (pH 8) to establish a pH gradient of 7–8 across the LUVs. Monitoring pH-dependent changes in the fluorescence intensity of HPTS allows us to compare the ion-transport abilities of the channels.

Although **A10** demonstrates excellent ion transport activity of 81% at 10 μM (Fig. 2a), varying the extravesicular salt from LiCl to CsCl surprisingly yields no significant differences (ranging from 76% to 83%) in transport activity. This finding suggests that **A10** likely facilitates the transmembrane transport of either anions or protons, rather than cations. Even more surprisingly, molecules **B10** and **C10** exhibit no detectable activity at the same concentration when the extravesicular salt was also varied from LiCl to CsCl. At present, we are unable to provide an explanation for this observation. These findings suggest that the dibenzo-12-crown-4 group may simply act as a pore-forming enhancer by strengthening side chain–side chain interactions and facilitating pore formation in lipid bilayers through oligomerization, akin to the pore-

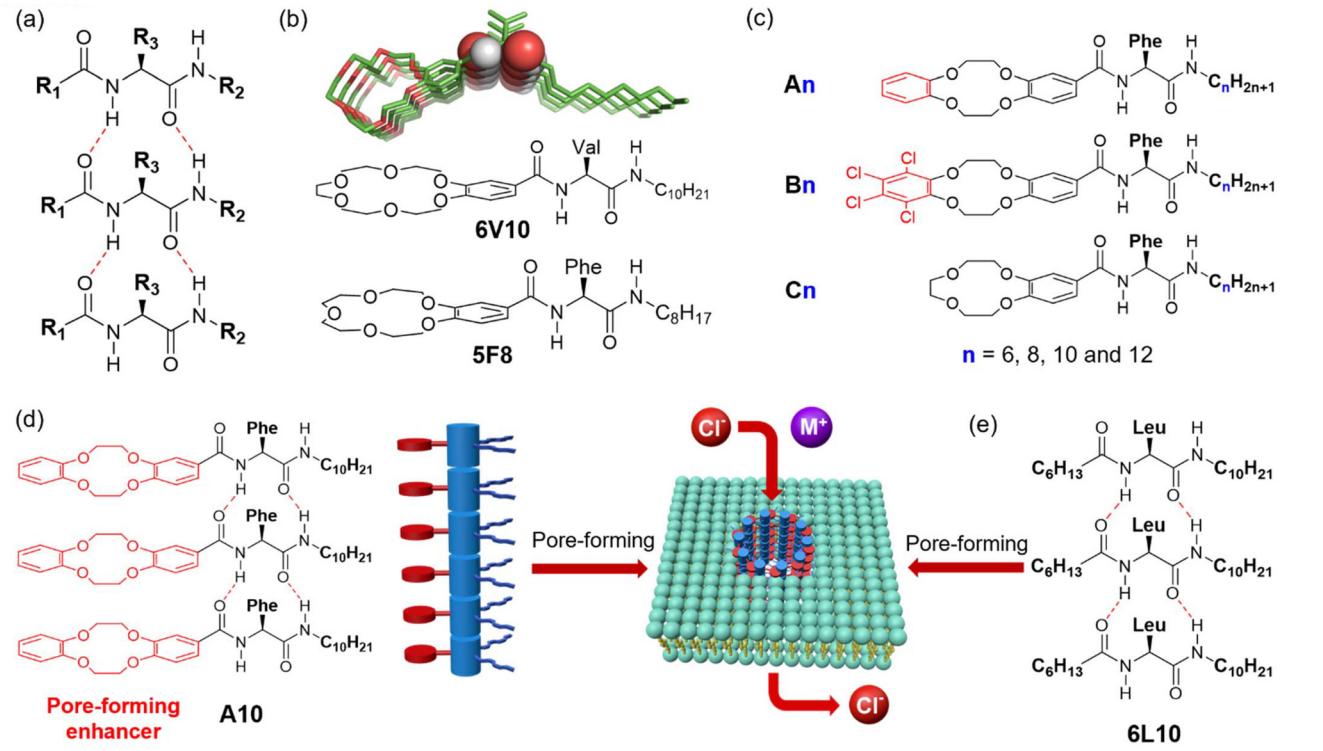

Fig. 1 (a) Monopeptide scaffold for aligning side chains of the same type (*e.g.* R_1–R_3) at the same side. (b) Crystal structure of **6V10** (top view) and molecular structures of **6V10** and **5F8**, demonstrating that the ability of the scaffold to form a H-bonded 1D columnar stack that aligns the crown ether to the same side. (c) The combinatorial construction of L-phenylalanine-derived molecules for the intended discovery of artificial Li^+ channels. (d) The dibenzo-12-crown-4 group unexpectedly serves as a pore-forming enhancer to strengthen the side chain–side chain interactions between 1D H-bonded stacks to form pores in a way like pore-forming **6L10** shown in (e) that assembles through side chain–side chain interactions to create pores in the membrane for Cl^- transport.

This journal is © the Partner Organisations 2025

Published on 17 March 2025. Downloaded by FUZHOU UNIVERSITY LIBRARY on 10/20/2025 8:49:18 AM.

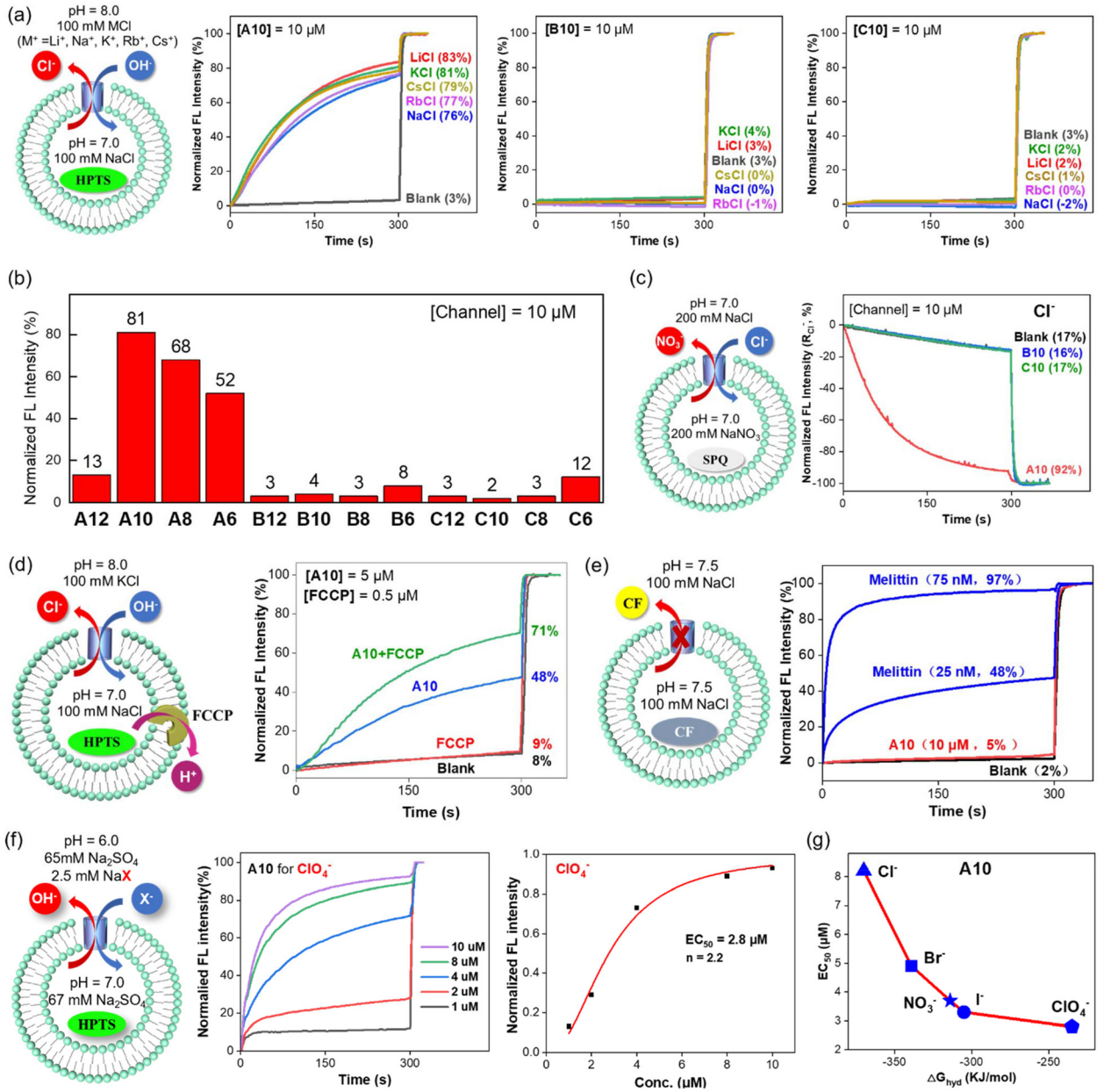

Fig. 2 (a) The ion-transport activities of **A10**, **B10** and **C10** in the presence of varied extravesicular metal salts determined using pH-sensitive HPTS assay. (b) Ion-transport activities of 12 **A*n*–C*n*** molecules (*n* = 6–12) determined using the HPTS assay, with the external region filled with 100 mM KCl. (c) The SPQ assay using the chloride-sensitive SPQ dye. (d) The HPTS assay in the presence of proton carrier FCCP to assess the relative transport rates between Cl^- and OH^-. (e) The CF dye assay to evaluate the membrane integrity in the presence of **A10**. (f) Determinatoin of EC_{50} value for **A10**-mediated transport of ClO_4^-. (g) EC_{50} values *vs.* hydration energies for **A10**-mediated transport of ClO_4^-, Cl^-, Br^-, I^-, and NO_3^-, determined in the presence of 2.5 mM NaX (X^- = Cl^-, Br^-, I^-, NO_3^-, and ClO_4^-) with proton gradient from pH = 7 (inside) to pH = 6 (outside). HPTS = (8-hydroxypyrene-1,3,6-trisulfonic acid); SPQ = 6-methoxy-*N*-(3-sulfopropyl); FCCP = carbonyl cyanide 4-(trifluoromethoxy) phenylhydrazone; CF = 5/6-carboxyfluorescein. [Total lipid] = 97.5 μM.

forming behaviour of molecule **6L10** and its other analogues, which we recently reported (Fig. 1e).[54,55]

A systematic scan of 12 molecules of **A*n*–C*n*** (*n* = 6, 8, 10, 12) identifies **A10** as the top performer (Fig. 2b). Hill analysis determines the EC_{50} value of **A10** for achieving 50% transmembrane activity to be 5.2 μM or 5.3 mol% relative to lipids (Fig. S3d†). For comparison, the well-established pore former **6L10**[54] exhibits an EC_{50} value of 4.3 μM (Fig. S3e†).

To examine the hypothesis that **A10** predominantly mediates chloride ion or proton transport, we conducted a Cl^--sensitive SPQ assay, which measures fluorescence quenching in the presence of Cl^- ions. By diluting $NaNO_3$-encapsulated LUVs into a NaCl buffer to establish a chloride gradient between the intravesicular and extravesicular medium, we observe high fluorescence quenching of SPQ by 92% (Fig. 2c). This result highlights the remarkable ability of **A10** to trans-

Published on 17 March 2025. Downloaded by FUZHOU UNIVERSITY LIBRARY on 10/20/2025 8:49:18 AM.

port Cl^- ions across the membrane. In line with the HPTS assay, the SPQ assay reveals no ion transport activity for **B10** and **C10** (Fig. 2c).

Given the observed ion transport behavior, the possibility of **A10** mediating alkali metal transport across the membrane is less likely. Thus, we can confidently assert that the predominant mechanism of **A10**-mediated ion transport is either Cl^-/OH^- antiport or Cl^-/H^+ symport, rather than M^+/H^+ antiport or M^+/OH^- symport. Furthermore, **A10**, composed of decyl chains with many slightly positively charged H-atoms (Fig. 1d), interacts more favorably, though weakly, with anions or the O-atoms from water molecules in the anion's hydration shell, rather than with cations/protons or their hydrated forms. As a result, the pore formed by **A10** is expected to facilitate preferential anion transport across the membrane. Therefore, it is reasonable to deduce that hydrated OH^- ions are transported more readily than hydrated H^+ ions through the pore. This suggests that Cl^-/OH^- antiport is more likely than H^+/Cl^- symport.

FCCP, a highly active H^+ carrier, was used to compare ion transport rates between Cl^- and OH^-. When FCCP was applied at 0.5 μM, the transport rate is nearly identical to the blank value, indicating that FCCP alone does not influence the system's ion transport activity. For **A10**, the transport efficiency increases from 48% without FCCP to 71% with FCCP, suggesting a significant synergistic effect between **A10** and FCCP. This implies that the transport rate of Cl^- is faster than that of OH^- (Fig. 2d), with the accumulated OH^- more quickly dispatched by FCCP through proton transport.

To determine whether the ion transmembrane activity is caused by membrane lysis induced by **A10**, an assay utilizing 5/6-CF molecules—measuring 9.2 Å × 11.4 Å and 10 Å × 10 Å—was conducted. This dye undergoes fluorescence quenching due to self-dimerization at high concentrations but exhibits stronger fluorescence intensity upon partial dissociation of self-dimers when the dye leaks into the extravesicular region. The addition of **A10** at 10 μM causes only a 5% increase in fluorescence intensity, whereas the same concentration of **A10** results in an 83% increase in the HPTS assay. In contrast, melittin, which forms pores larger than 1 nm, causes a 48% increase in fluorescence intensity at 25 nM and a 97% increase at 75 nM (Fig. 2e). These results indicate that the membrane integrity was not compromised in the presence of **A10**, and the pores formed by **A10** in the lipid bilayer are less than 1 nm in diameter.

The anion transport selectivity of **A10** for Cl^-, Br^-, I^-, NO_3^-, and ClO_4^- was evaluated using a HPTS-based assay. In brief, the LUVs encapsulated 67 mM Na_2SO_4, with its extravesicular region containing 65 mM Na_2SO_4 and 2.5 mM NaX (where X^- = Cl^-, Br^-, I^-, NO_3^-, ClO_4^-) with a proton gradient from pH 7 (inside) to pH 6 (outside). Comparison of EC_{50} values determined for the five anions using Hill plots indicates that the anion transport selectivity of **A10** follows the order: $ClO_4^- > I^- > NO_3^- > Br^- > Cl^-$ (Fig. 2f, g and S4†). This selectivity corresponds with the decreasing hydration energy of the anions. This result suggests that the mechanism for anion transmembrane transport likely involves the removal of water molecules surrounding anions.

To investigate the transport mechanism of **A10**, single-channel current traces were recorded at various voltages using a planar lipid bilayer containing 1 M KCl solutions in symmetric baths (Fig. 3a). The recorded single-channel current traces clearly demonstrate that **A10**-mediated transmembrane chloride transport occurs through a channel mechanism rather than a carrier mechanism. A linear Ohmic curve was obtained from fitting the current–voltage (*I–V*) plot, yielding the Cl^- conductance (γ_{Cl^-}) value of 2.29 ± 0.06 pS for **A10** (Fig. 3a). Additionally, asymmetric baths (*cis* chamber = 1.0 M KCl and *trans* chamber = 0.5 M KCl) were used to evaluate the Cl^-/K^+ transport selectivity. Substituting the reverse potential of 20.3 mV from the *I–V* curve (Fig. 3d and S5†) into the Goldman–Hodgkin–Katz equation gave the Cl^-/K^+ transport selectivity of 17, confirming **A10**'s strong preference for anions over cations.

The above findings provide definitive experimental evidence through the HPTS assay and single-channel current measurements that clearly demonstrate the formation of structured channels for **A10**, enabling anion transport across lipid membranes. Nevertheless, the precise determination of the pore structures and the exact process of pore formation remains elusive, posing considerable challenges both experimentally and computationally. To at least offer some speculative insights into the potential structural characteristics of the one-dimensional alignment of **A10** within the lipid membrane, we carried out molecular dynamics (MD) simulation of $(\mathbf{A10})_6$ in DOPC membrane to help illuminate aspects of pore formation in synthetic ion channels. H-bonded $(\mathbf{A10})_6$ was first optimized using the M06-2X/6-31G(d) level of theory (Fig. 3c), which was then subjected to MD simulation for 200 ns. A closer examination of 2000 structural snapshots in the last 10 ns of trajectories reveals a key observation: all six **A10** molecules consistently maintained H-bonding with each other across all 2000 structures, confirming the stability of the intermolecular H-bonds that enable the formation of a stable, H-bonded one-dimensional structure capable of spanning the hydrophobic membrane region (Fig. 3d).

Lastly, to explore why crown ether groups do not facilitate ion transport, we conducted picrate extraction experiments to determine the binding constants of **A*n***s toward Li^+, Na^+ and K^+ ions. As summarized in Table 1, all **A*n***s exhibit binding constants of less than 153 M^{-1} toward Li^+, Na^+ or K^+ ions. Considering that the dynamic transmembrane ion transport process requires channel molecules to effectively capture and release ions, the binding affinity between channel molecules and ions plays a crucial role in this process. If the binding is too strong, ion release might get hindered; if too weak, ion capture becomes inefficient. According to our previous report on 15-crown-5-containing channel molecules structurally similar to **A*n***s,[54] (1) efficient ion transport occurs when the binding constants between channel molecules and alkali metal ions range from 4.2×10^2 and 8.2×10^2 M^{-1}, effectively facilitating both ion capture and lease, (2) transport activity

 This journal is © the Partner Organisations 2025

Published on 17 March 2025. Downloaded by FUZHOU UNIVERSITY LIBRARY on 10/20/2025 8:49:18 AM.

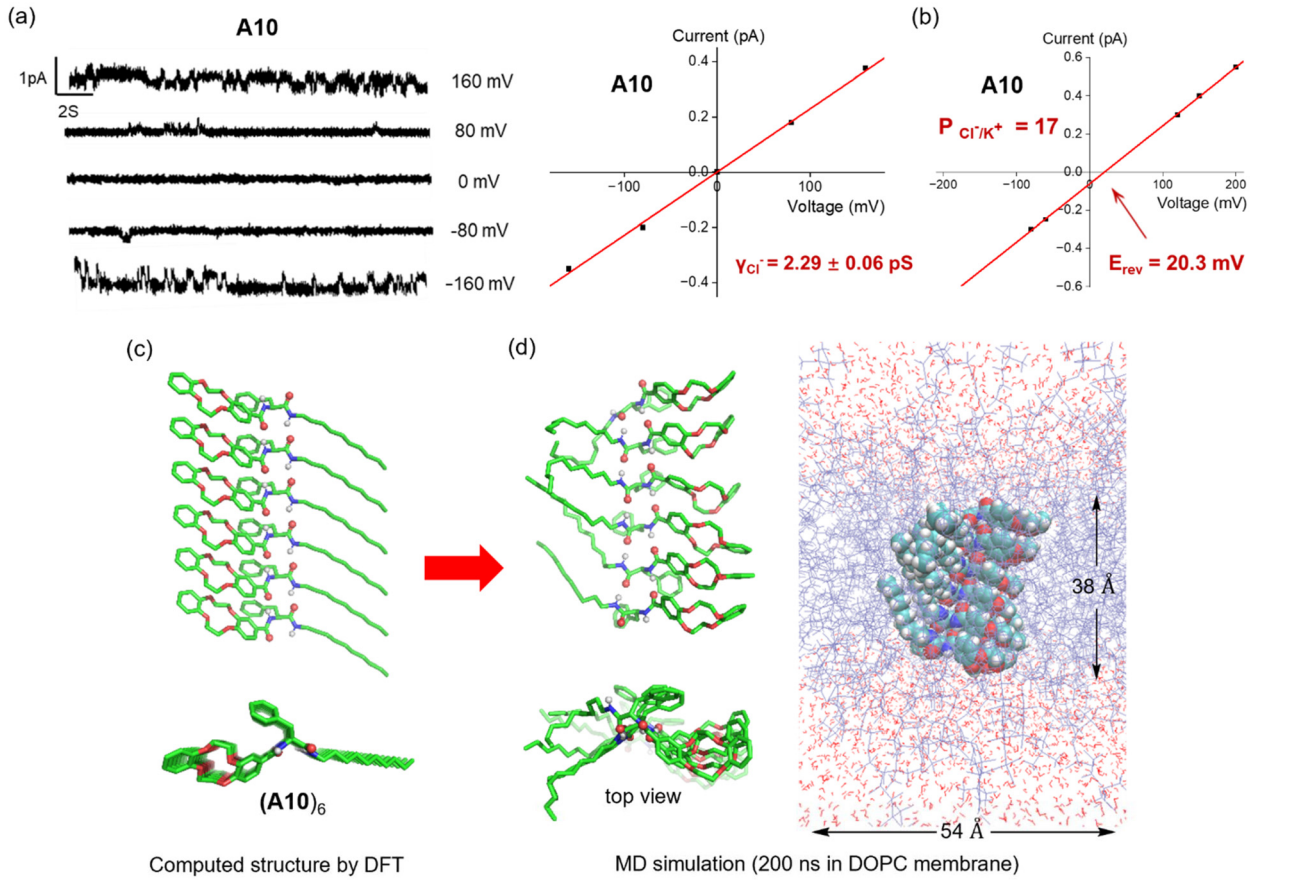

Fig. 3 (a) Single-channel current traces recorded in symmetric baths (*cis* chamber = *trans* chamber = 1 M KCl) for **A10** and determination of Cl^- conductance (γ_{Cl^-}) using a linear ohmic current–voltage (*I*–*V*). (b) The Cl^-/K^+ selectivity of **A10** determined from the reverse potential (20.3 mV), which is obtained from fitting the plots recorded in asymmetric bath (*cis* chamber = 1.0 M KCl and *trans* chamber = 0.5 M KCl). (c) The structure of $(\mathbf{A10})_6$ was optimized at the M06-2X/6-31G(d) level of DFT theory under periodic boundary conditions in the gas phase. (d) The DFT-derived structure was subjected to MD simulation in a DOPC membrane, revealing an intact H-bonded network that confirms the stability of H-bonds in the membrane. DOPC = 1,2-dioleoyl-*sn*-*glycero*-3-phosphocholine.

Table 1 Binding constants (K_a) between **A*n*** (*n* = 6–12) and Li^+, Na^+ or K^+ ions at 25 °C obtained using Cram's method[a]

	K_a (Li^+, M^{-1})	K_a (Na^+, M^{-1})	K_a (K^+, M^{-1})
A6	1.08×10^2	1.11×10^2	0.72×10^2
A8	0.89×10^2	0.98×10^2	0.48×10^2
A10	1.53×10^2	0.80×10^2	0.60×10^2
A12	0.91×10^2	0.84×10^2	0.58×10^2

[a] Determined based on the partition of 10 mM alkali picrate salts in 1 mL H_2O into 1 mL of $CHCl_3$ containing 10 mM **A*n*** and the assumption of 1 : 1 complex formation.

roughly increases with increasing binding constants within this range, and (3) when the binding constant exceeds 1.5×10^3 M^{-1}, ion release becomes significantly restricted, impeding transmembrane ion transport. From these findings, weak binding constants of less than 153 M^{-1} exhibited by all **A*n*s** may indicate inefficient ion capturing from the aqueous solution, which consequently results in the absence of experimentally observable ion transport.

Conclusions

To summarize, we have established here a relatively novel approach to pore formation in lipid bilayers through the assistance of a rigid dibenzo-12-crown-4 moiety. Although these rigid 12-crown-4 units are vertically arrayed on top of each other induced by the H-bonded one-dimensional stack, they do not transport cations as expected. Rather, they appear to merely serve as a pore-forming enhancer, strengthening the side chain–side chain interactions between the 1D stacks and subsequently resulting in pores less than 1 nm. The formed pores, characterized by a slight positive charge on their luminal surfaces due to the alignment of H-atoms along the inner pore surface, efficiently facilitate anion transport across the membrane through a channel mechanism. This configuration results in a high Cl^-/K^+ transport selectivity of 17, highlighting the exceptional anion selectivity of the pore and its promising potential for further exploration in biomimetic chemistry for targeted ion transport applications. This study exemplifies how simple synthetic molecules can yield unex-

Published on 17 March 2025. Downloaded by FUZHOU UNIVERSITY LIBRARY on 10/20/2025 8:49:18 AM.

pected functions, providing valuable insights into the structure–function relationship of ion channels, deepening our understanding of the principles governing ion channel behaviour.

Data availability

All relevant data are within the manuscript and its ESI.†

Conflicts of interest

There are no conflicts to declare.

Acknowledgements

This work is supported by the National Natural Science Foundation of China (22271049 and 22371048), Natural Science Foundation of Fujian Province (2023J01054) and a start-up grant from Fuzhou University.

References

1 C. A. Hübner and T. J. Jentsch, Ion channel diseases, *Hum. Mol. Genet.*, 2002, **11**, 2435–2445.
2 M. A. Zaydman, J. R. Silva and J. Cui, Ion Channel Associated Diseases: Overview of Molecular Mechanisms, *Chem. Rev.*, 2012, **112**, 6319–6333.
3 K. Berend, L. H. van Hulsteijn and R. O. B. Gans, Chloride: The queen of electrolytes?, *Eur. J. Intern. Med.*, 2012, **23**, 203–211.
4 J. T. Davis, O. Okunola and R. Quesada, Recent advances in the transmembrane transport of anions, *Chem. Soc. Rev.*, 2010, **39**, 3843–3862.
5 P. R. Brotherhood and A. P. Davis, Steroid-based anion receptors and transporters, *Chem. Soc. Rev.*, 2010, **39**, 3633–3647.
6 K. Steinmeyer, C. Ortland and T. J. Jentsch, Primary structure and functional expression of a developmentally regulated skeletal muscle chloride channel, *Nature*, 1991, **354**, 301–304.
7 D. C. Gadsby, P. Vergani and L. Csanády, The ABC protein turned chloride channel whose failure causes cystic fibrosis, *Nature*, 2006, **440**, 477–483.
8 M. A. Mall and L. J. V. Galietta, Targeting ion channels in cystic fibrosis, *J. Cystic Fibrosis*, 2015, **14**, 561–570.
9 L. Puljak and G. Kilic, Emerging roles of chloride channels in human diseases, *Biochim. Biophys. Acta, Mol. Basis Dis.*, 2006, **1762**, 404–413.
10 J. Yang, G. Yu, J. L. Sessler, I. Shin, P. A. Gale and F. Huang, Artificial transmembrane ion transporters as potential therapeutics, *Chem*, 2021, **7**, 3256–3291.
11 E. C. Cooper and L. Y. Jan, Ion channel genes and human neurological disease: Recent progress, prospects, and challenges, *Proc. Natl. Acad. Sci. U. S. A.*, 1999, **96**, 4759–4766.
12 S. Bajaj, S. T. Ong and K. G. Chandy, Contributions of natural products to ion channel pharmacology, *Nat. Prod. Rep.*, 2020, **37**, 703–716.
13 E. N. W. Howe, V.-V. T. Chang, X. Wu, M. Fares, W. Lewis, L. K. Macreadie and P. A. Gale, Halide-selective, proton-coupled anion transport by phenylthiosemicarbazones, *Biochim. Biophys. Acta, Mol. Basis Dis.*, 2022, **1864**, 183828.
14 M. R. Ghadiri, J. R. Granja and L. K. Buehler, Artificial transmembrane ion channels from self-assembling peptide nanotubes, *Nature*, 1994, **369**, 301–304.
15 T. M. Fyles, Synthetic ion channels in bilayer membranes, *Chem. Soc. Rev.*, 2007, **36**, 335–347.
16 C. Ren, X. Ding, A. Roy, J. Shen, S. Zhou, F. Chen, S. F. Yau Li, H. Ren, Y. Y. Yang and H. Q. Zeng, A halogen bond-mediated highly active artificial chloride channel with high anticancer activity, *Chem. Sci.*, 2018, **9**, 4044–4051.
17 A. Mondal, S. N. Save, S. Sarkar, D. Mondal, J. Mondal, S. Sharma and P. Talukdar, A Benzohydrazide-Based Artificial Ion Channel that Modulates Chloride Ion Concentration in Cancer Cells and Induces Apoptosis by Disruption of Autophagy, *J. Am. Chem. Soc.*, 2023, **145**, 9737–9745.
18 J. C. Nelson, J. G. Saven, J. S. Moore and P. G. Wolynes, Solvophobically Driven Folding of Nonbiological Oligomers, *Science*, 1997, **277**, 1793–1796.
19 W.-H. Chen, X.-B. Shao and S. L. Regen, Poly(choloyl)-Based Amphiphiles as Pore-Forming Agents: Transport-Active Monomers by Design, *J. Am. Chem. Soc.*, 2005, **127**, 12727–12735.
20 T. Muraoka, T. Shima, T. Hamada, M. Morita, M. Takagi, K. V. Tabata, H. Noji and K. Kinbara, Ion Permeation by a Folded Multiblock Amphiphilic Oligomer Achieved by Hierarchical Construction of Self-Assembled Nanopores, *J. Am. Chem. Soc.*, 2012, **134**, 19788–19794.
21 T. Muraoka, T. Endo, K. V. Tabata, H. Noji, S. Nagatoishi, K. Tsumoto, R. Li and K. Kinbara, Reversible Ion Transportation Switch by a Ligand-Gated Synthetic Supramolecular Ion Channel, *J. Am. Chem. Soc.*, 2014, **136**, 15584–15595.
22 T. Muraoka, D. Noguchi, R. S. Kasai, K. Sato, R. Sasaki, K. V. Tabata, T. Ekimoto, M. Ikeguchi, K. Kamagata, N. Hoshino, H. Noji, T. Akutagawa, K. Ichimura and K. Kinbara, A synthetic ion channel with anisotropic ligand response, *Nat. Commun.*, 2020, **11**, 2924.
23 G. Das, P. Talukdar and S. Matile, Fluorometric Detection of Enzyme Activity with Synthetic Supramolecular Pores, *Science*, 2002, **298**, 1600–1602.
24 A. J. Helsel, A. L. Brown, K. Yamato, W. Feng, L. Yuan, A. J. Clements, S. V. Harding, G. Szabo, Z. Shao and B. Gong, Highly Conducting Transmembrane Pores Formed by Aromatic Oligoamide Macrocycles, *J. Am. Chem. Soc.*, 2008, **130**, 15784–15785.
25 J. Shen, Y. Gu, L. Ke, Q. Zhang, Y. Cao, Y. Lin, Z. Wu, C. Wu, Y. Mu, Y.-L. Wu, C. Ren and H. Q. Zeng,

 This journal is © the Partner Organisations 2025

Published on 17 March 2025. Downloaded by FUZHOU UNIVERSITY LIBRARY on 10/20/2025 8:49:18 AM.

Cholesterol-stabilized membrane-active nanopores with anticancer activities, *Nat. Commun.*, 2022, **13**, 5985.

26 L. Ma, M. Melegari, M. Colombini and J. T. Davis, Large and Stable Transmembrane Pores from Guanosine–Bile Acid Conjugates, *J. Am. Chem. Soc.*, 2008, **130**, 2938–2939.

27 N. Sakai, J. Mareda and S. Matile, Rigid-Rod Molecules in Biomembrane Models: From Hydrogen-Bonded Chains to Synthetic Multifunctional Pores, *Acc. Chem. Res.*, 2005, **38**, 79–87.

28 N. Sakai, J. Mareda and S. Matile, Artificial β-Barrels, *Acc. Chem. Res.*, 2008, **41**, 1354–1365.

29 N. Yoshino, A. Satake and Y. Kobuke, An Artificial Ion Channel Formed by a Macrocyclic Resorcin[4]arene with Amphiphilic Cholic Acid Ether Groups, *Angew. Chem., Int. Ed.*, 2001, **40**, 457–459.

30 C. Goto, M. Yamamura, A. Satake and Y. Kobuke, Artificial Ion Channels Showing Rectified Current Behavior, *J. Am. Chem. Soc.*, 2001, **123**, 12152–12159.

31 J. Zhang, B. Jing and S. L. Regen, Kinetic Evidence for the Existence and Mechanism of Formation of a Barrel Stave Structure from Pore-Forming Dendrimers, *J. Am. Chem. Soc.*, 2003, **125**, 13984–13987.

32 X. Zhou, G. Liu, K. Yamato, Y. Shen, R. Cheng, X. Wei, W. Bai, Y. Gao, H. Li, Y. Liu, F. Liu, D. M. Czajkowsky, J. Wang, M. J. Dabney, Z. Cai, J. Hu, F. V. Bright, L. He, X. C. Zeng, Z. Shao and B. Gong, Self-assembling subnanometer pores with unusual mass-transport properties, *Nat. Commun.*, 2012, **3**, 949.

33 X. Wei, G. Zhang, Y. Shen, Y. Zhong, R. Liu, N. Yang, F. Y. Al-mkhaizim, M. A. Kline, L. He, M. Li, Z.-L. Lu, Z. Shao and B. Gong, Persistent Organic Nanopores Amenable to Structural and Functional Tuning, *J. Am. Chem. Soc.*, 2016, **138**, 2749–2754.

34 Z. Chen, X. Xie, C. Jia, Q. Zhong, Q. Zhang, D. Luo, Y. Cao, Y. Mu and C. Ren, Concentration-Driven Evolution of Adaptive Artificial Ion Channels or Nanopores with Specific Anticancer Activities, *Angew. Chem., Int. Ed.*, 2024, **63**, e202318811.

35 N. Sakai, Y. Kamikawa, M. Nishii, T. Matsuoka, T. Kato and S. Matile, Dendritic Folate Rosettes as Ion Channels in Lipid Bilayers, *J. Am. Chem. Soc.*, 2006, **128**, 2218–2219.

36 T. Saha, S. Dasari, D. Tewari, A. Prathap, K. M. Sureshan, A. K. Bera, A. Mukherjee and P. Talukdar, Hopping-Mediated Anion Transport through a Mannitol-Based Rosette Ion Channel, *J. Am. Chem. Soc.*, 2014, **136**, 14128–14135.

37 R. N. Das, Y. P. Kumar, O. M. Schütte, C. Steinem and J. Dash, A DNA-Inspired Synthetic Ion Channel Based on G–C Base Pairing, *J. Am. Chem. Soc.*, 2015, **137**, 34–37.

38 M. Debnath, S. Chakraborty, Y. P. Kumar, R. Chaudhuri, B. Jana and J. Dash, Ionophore constructed from non-covalent assembly of a G-quadruplex and liponucleoside transports K^+-ion across biological membranes, *Nat. Commun.*, 2020, **11**, 469.

39 P. Tripathi, L. Shuai, H. Joshi, H. Yamazaki, W. H. Fowle, A. Aksimentiev, H. Fenniri and M. Wanunu, Rosette Nanotube Porins as Ion Selective Transporters and Single-Molecule Sensors, *J. Am. Chem. Soc.*, 2020, **142**, 1680–1685.

40 J. Shen, R. Ye, Z. Liu and H. Q. Zeng, Hybrid Pyridine–Pyridone Foldamer Channels as M2-Like Artificial Proton Channels, *Angew. Chem., Int. Ed.*, 2022, **61**, e202200259.

41 A. Roy, H. Joshi, R. Ye, J. Shen, F. Chen, A. Aksimentiev and H. Q. Zeng, Polyhydrazide-Based Organic Nanotubes as Efficient and Selective Artificial Iodide Channels, *Angew. Chem., Int. Ed.*, 2020, **59**, 4806–4813.

42 F. Chen, J. Shen, N. Li, A. Roy, R. Ye, C. Ren and H. Q. Zeng, Pyridine/Oxadiazole-Based Helical Foldamer Ion Channels with Exceptionally High K^+/Na^+ Selectivity, *Angew. Chem., Int. Ed.*, 2020, **59**, 1440–1444.

43 J. Shen, R. Ye, A. Romanies, A. Roy, F. Chen, C. Ren, Z. Liu and H. Q. Zeng, Aquafoldmer-Based Aquaporin-like Synthetic Water Channel, *J. Am. Chem. Soc.*, 2020, **142**, 10050–10058.

44 J. Shen, D. R. Z. Li, H. Oh, H. Behera, H. Joshi, M. Kumar, A. Aksimentiev and H. Q. Zeng, Sulfur-Containing Foldamer-Based Artificial Lithium Channels, *Angew. Chem., Int. Ed.*, 2023, **62**, e202305623.

45 J. Shen, A. Roy, H. Joshi, L. Samineni, R. Ye, Y.-M. Tu, W. Song, M. Skiles, M. Kumar, A. Aksimentiev and H. Q. Zeng, Fluorofoldamer-Based Salt- and Proton-Rejecting Artificial Water Channels for Ultrafast Water Transport, *Nano Lett.*, 2022, **22**, 4831–4838.

46 A. Roy, J. Shen, H. Joshi, W. Song, Y.-M. Tu, R. Chowdhury, R. Ye, N. Li, C. Ren, M. Kumar, A. Aksimentiev and H. Q. Zeng, Foldamer-based ultrapermeable and highly selective artificial water channels that exclude protons, *Nat. Nanotechnol.*, 2021, **16**, 911–917.

47 T. Yan, S. Liu, J. Xu, H. Sun, S. Yu and J. Liu, Unimolecular Helix-Based Transmembrane Nanochannel with a Smallest Luminal Cavity of 1 Å Expressing High Proton Selectivity and Transport Activity, *Nano Lett.*, 2021, **21**, 10462–10468.

48 H. Chen, Y. Liu, X. Cheng, S. Fang, Y. Sun, Z. Yang, W. Zheng, X. Ji and Z. Wu, Self-Assembly of Size-Controlled m-Pyridine–Urea Oligomers and Their Biomimetic Chloride Ion Channels, *Angew. Chem., Int. Ed.*, 2021, **60**, 10833–10841.

49 L. Zhang, C. Zhang, X. Dong and Z. Dong, Highly Selective Transmembrane Transport of Exogenous Lithium Ions through Rationally Designed Supramolecular Channels, *Angew. Chem., Int. Ed.*, 2023, **62**, e202214194.

50 S. Qi, C. Zhang, H. Yu, J. Zhang, T. Yan, Z. Lin, B. Yang and Z. Dong, Foldamer-Based Potassium Channels with High Ion Selectivity and Transport Activity, *J. Am. Chem. Soc.*, 2021, **143**, 3284–3288.

51 Z. Ajmal, M. Arif, A. Kumar, M. U. Haq, Y. Du, Y. Zhang, M. Abboud, J. Qian, Z. Chen, B.-J. Ni and H. Q. Zeng, Uniformaly distributed Ru nanoparticles over N, P co-doped porous carbon as a highly active trifunctional electrocatalyst, *Int. J. Hydrogen Energy*, 2024, **73**, 768–774.

52 C. Lang, X. Deng, F. Yang, B. Yang, W. Wang, S. Qi, X. Zhang, C. Zhang, Z. Dong and J. Liu, Highly Selective Artificial Potassium Ion Channels Constructed from Pore-

Published on 17 March 2025. Downloaded by FUZHOU UNIVERSITY LIBRARY on 10/20/2025 8:49:18 AM.

Containing Helical Oligomers, *Angew. Chem., Int. Ed.*, 2017, **56**, 12668–12671.

53 J. E. Jones, V. Diemer, C. Adam, J. Raftery, R. E. Ruscoe, J. T. Sengel, M. I. Wallace, A. Bader, S. L. Cockroft, J. Clayden and S. J. Webb, Length-Dependent Formation of Transmembrane Pores by 310-Helical α-Aminoisobutyric Acid Foldamers, *J. Am. Chem. Soc.*, 2016, **138**, 688–695.

54 C. L. Ren, F. Zeng, J. Shen, F. Chen, A. Roy, S. Zhou, H. Ren and H. Q. Zeng, Pore-Forming Monopeptides as Exceptionally Active Anion Channels, *J. Am. Chem. Soc.*, 2018, **140**, 8817–8826.

55 F. Zeng, F. Liu, L. Yuan, S. Zhou, J. Shen, N. Li, H. Ren and H. Q. Zeng, A Pore-Forming Tripeptide as an Extraordinarily Active Anion Channel, *Org. Lett.*, 2019, **21**, 4826–4830.

56 L. Yuan, J. Shen, R. J. Ye, F. Chen and H. Q. Zeng, Structurally simple trimesic amides as highly selective anion channels, *Chem. Commun.*, 2019, **55**, 4797–4800.

57 A. D. Peters, S. Borsley, F. della Sala, D. F. Cairns-Gibson, M. Leonidou, J. Clayden, G. F. S. Whitehead, I. J. Vitórica-Yrezábal, E. Takano, J. Burthem, S. L. Cockroft and S. J. Webb, Switchable foldamer ion channels with antibacterial activity, *Chem. Sci.*, 2020, **11**, 7023–7030.

58 C. Dutta, P. Krishnamurthy, D. Su, S. H. Yoo, G. W. Collie, M. Pasco, J. K. Marzinek, P. J. Bond, C. Verma, A. Grélard, A. Loquet, J. Li, M. Luo, M. Barboiu, G. Guichard, R. M. Kini and P. P. Kumar, Nature-inspired synthetic oligourea foldamer channels allow water transport with high salt rejection, *Chem*, 2023, **9**, 2237–2254.

59 S. Deng, Z. Li, L. Yuan and H. Q. Zeng, An Exceptionally Active and Highly Selective Perchlorate Transporter Containing a Trimesic Amide Scaffold, *Molecules*, 2024, **29**, 1118.

60 C. Ren, F. Chen, F. Zhou, J. Shen, H. Su and H. Q. Zeng, Low-Cost Phase-Selective Organogelators for Rapid Gelation of Crude Oils at Room Temperature, *Langmuir*, 2016, **32**, 13510–13516.

61 C. Ren, J. Shen, F. Chen and H. Q. Zeng, Rapid Room-Temperature Gelation of Crude Oils by a Wetted Powder Gelator, *Angew. Chem., Int. Ed.*, 2017, **56**, 3847–3851.

62 J. Li, Y. Huo and H. Q. Zeng, Combinatorial identification of a highly soluble phase-selective organogelator with high gelling capacity for crude oil gelation, *J. Mater. Chem. A*, 2018, **6**, 10196–10200.

63 J. Li, Y. Huo and H. Q. Zeng, Polar Solvent-Induced Unprecedented Supergelation of (Un)Weathered Crude Oils at Room Temperature, *Langmuir*, 2018, **34**, 8058–8064.

64 J. Shen, R. Ye and H. Q. Zeng, Crystal Packing-Guided Construction of Hetero-Oligomeric Peptidic Ensembles as Synthetic 3-in-1 Transporters, *Angew. Chem., Int. Ed.*, 2021, **60**, 12924–12930.

65 C. Ren, J. Shen and H. Q. Zeng, Combinatorial Evolution of Fast-Conducting Highly Selective K^+-Channels via Modularly Tunable Directional Assembly of Crown Ethers, *J. Am. Chem. Soc.*, 2017, **139**, 12338–12341.

66 L. Jin, C. Sun, Z. Li, J. Shen and H. Q. Zeng, A K^+-selective channel with a record-high K^+/Na^+ selectivity of 20.1, *Chem. Commun.*, 2023, **59**, 3610–3613.

67 L. Yuan, P. Jiang, J. Hu, H. Zeng, Y. Huo, Z. Li and H. Q. Zeng, A highly active and selective chalcogen bond-mediated perchlorate channel, *Chin. Chem. Lett.*, 2022, **33**, 2026–2030.

68 H. Ma, R. Ye, L. Jin, S. Zhou, C. Ren, H. Ren, J. Shen and H. Q. Zeng, Highly active artificial potassium channels having record-high K^+/Na^+ selectivity of 20.1, *Chin. Chem. Lett.*, 2023, **34**, 108355.

69 L. Z. Zeng, H. Zhang, T. Wang and T. Li, Enhancing K^+ transport activity and selectivity of synthetic K^+ channels via electron-donating effects, *Chem. Commun.*, 2020, **56**, 1211–1214.

 This journal is © the Partner Organisations 2025